NJC

LETTER

View Article Online
View Journal | View Issue

Multigram synthesis of bis[(trimethylsilyl)ethynyl]benzenes suitable for post-polymerization modification†

Cite this: *New J. Chem.*, 2014, 38, 2229

Received (in Montpellier, France) 2nd January 2014,
Accepted 3rd March 2014

DOI: 10.1039/c4nj00011k

www.rsc.org/njc

Florian Glöcklhofer,[a] Daniel Lumpi,*[a] Berthold Stöger[b] and Johannes Fröhlich[a]

Novel substituted bis[(trimethylsilyl)ethynyl]benzenes have been prepared as versatile building blocks for organic functional materials. The resulting effects of replacing sulfur by selenium and tellurium on photophysical and electrochemical properties have been examined. Polymerization *via* microwave-assisted Cu(I)-catalyzed azide–alkyne cycloaddition (CuAAC) and subsequent post-polymerization modification by oxidation reveals the utility of the developed building blocks.

1,4-Bis[(trimethylsilyl)ethynyl]-2,5-bis(hexyloxy)benzene (X = O) and the desilylated species 1,4-bis(ethynyl)-2,5-bis(hexyloxy)benzene are of current interest in the synthesis of a growing number of functional organic materials such as fluorescent polymers,[1] conjugated sensor materials,[2,3] conducting metallopolymers[4] and special materials like shape-persistent macrocycles.[5] In terms of further applications, the two alkyne groups enable the functionalization by a variety of established reactions such as alkyne metathesis,[6,7] Glaser coupling,[8] Sonogashira coupling,[9] azide–alkyne cycloaddition,[10] *etc.*

Despite the widespread utility of hexyloxy-substituted benzenes,[1–5] the synthesis of the sulfur, selenium and tellurium containing analogs **6a–c** has not been reported to date. However, replacing the oxygen atom by these elements may significantly affect the properties of the material, as reported for heterocyclic polymers polyfuran, -thiophene, -selenophene and -tellurophene. Whereas polyfuran has attracted less attention, polythiophenes are widely utilized due to their conducting properties.[11] Replacing sulfur by selenium in polythiophenes results in reduced bandgaps and lower LUMO energy levels, leading to ambipolar charge transport properties.[12] In contrast, characteristics of polytellurophenes are severely affected by Te–Te interactions, which are expected to result in strong interchain electronic coupling.[13]

We report on a straightforward, comparatively cheap and scalable synthesis of novel sulfur, selenium and tellurium based analogs (**6a–c**) of 1,4-bis[(trimethylsilyl)ethynyl]2,5-bis(hexyloxy)benzene. The introduction of these elements does not only impact the material properties but also allows for a specific modification of the photophysical and electrochemical characteristics by simple oxidation, which is demonstrated using the example of post-polymerization modification.

The discussion of the results is split into two subchapters: (1) the large-scale synthesis of novel building-blocks for functional organic polymers and (2) an exemplary application of the developed monomers in materials suitable for post-polymerization modification.

The synthetic pathway towards monomers **6a–c** is illustrated in Scheme 1. A multigram synthesis of 2,5-dibromobenzoquinone **3** from 1,4-dimethoxybenzene **1** was previously reported by López-Alvarado *et al.*[14] Following this procedure, the synthesis of **3** could be achieved on the 30 g scale (71%).

Nucleophilic addition[15] of TMS-acetylene applying *n*-BuLi resulted in an isomeric mixture of **4a** and **4b** (3 : 1 (*cis*/*trans*), not assigned) in a good yield of 85% (20 g). Since both isomers are converted to **5** at similar rates in the subsequent reductive aromatization, separation of the two isomers is not required. Nevertheless, the removal of impurities by filtration through a pad of silica and trituration in boiling *n*-hexane proved to be advantageous to avoid the cleavage of the TMS-group in the subsequent reduction step[15] to form **5**, which was accomplished in good yields of 94% (12 g) using $SnCl_2{\cdot}2H_2O$. The hexylthio-, hexylseleno- and hexyltelluro-groups were introduced by a lithium–halogen exchange and subsequent addition of either elemental sulfur or selenium and hexyl iodide to obtain **6a** (2.5 g, 63%) and **6b** (1.7 g, 73%) or dihexyl ditelluride[16] to obtain **6c** (1.5 g, 53%).

To ensure scalability, all steps toward **5** were carried out utilizing purification techniques such as extraction, crystallization, trituration and flash filtration through silica. **6a–c**

[a] *Institute of Applied Synthetic Chemistry, Vienna University of Technology, Getreidemarkt 9/163, A-1060 Vienna, Austria. E-mail: daniel.lumpi@tuwien.ac.at*
[b] *Institute of Chemical Technologies and Analytics, Vienna University of Technology, Getreidemarkt 9/164, A-1060 Vienna, Austria*

† Electronic supplementary information (ESI) available: Synthesis and characterization of all synthesized compounds as well as crystal structures and crystallographic information files (CIFs) for **6a**, **6b** and **6d**. CCDC 955488–955490. For ESI and crystallographic data in CIF or other electronic format see DOI: 10.1039/c4nj00011k

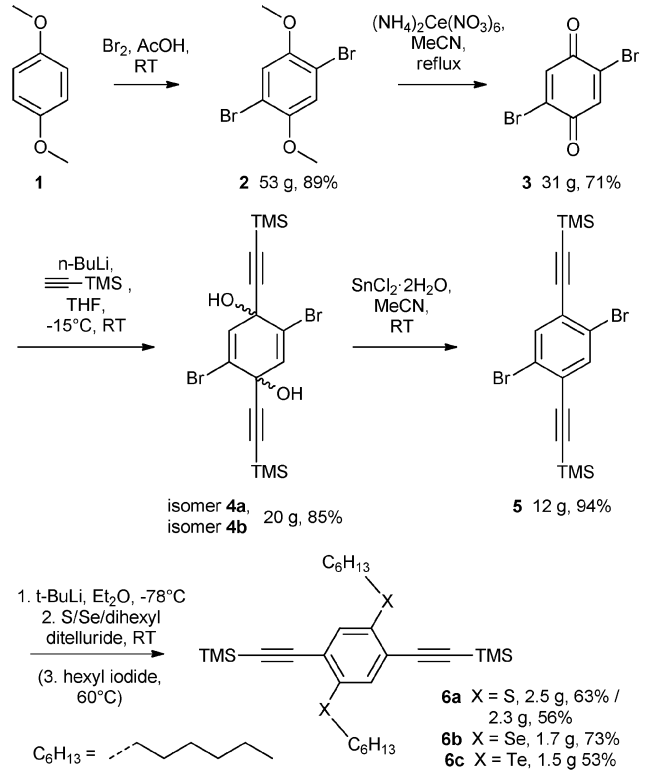

Scheme 1 Synthetic route towards monomers **6a–c**.

were purified by column chromatography; however, exemplarily **6a** was alternatively purified by crystallization, resulting in only slightly lower yields (56% instead of 63%).

An alternative modification approach to the heteroatom exchange (S/Se/Te) represents the possibility to modify molecular properties by selective oxidation of these elements. This enables us to directly convert the electron donating +M-substituent (*e.g.* alkylthio) to an electron accepting −M-substituent (*e.g.* sulfone), thus significantly influencing electrochemical and photophysical characteristics.

In order to evaluate convenient oxidation conditions the conversion of **6a** to sulfone **6d** was chosen as a model reaction (Scheme 2). Dimethyldioxirane (DMDO), a mild and versatile oxidation reagent, proved to be particularly advantageous with regard to purification, selectivity as well as efficiency (98%). With regard to the applicability of this oxidation reagent, our group reported on practical and efficient large-scale preparation of DMDO.[17]

Single crystals of **6a** and **6b** were obtained by solvent evaporation from *n*-hexane;[18] **6c** did not give suitable crystals. The crystal structure of **6a** is shown in Fig. 1.

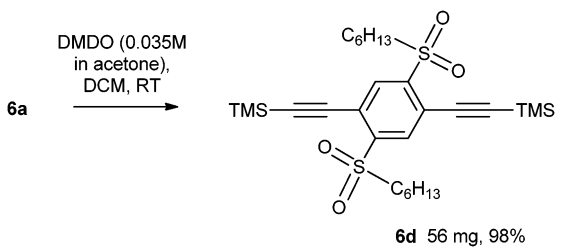

Scheme 2 Oxidation protocol towards **6d**.

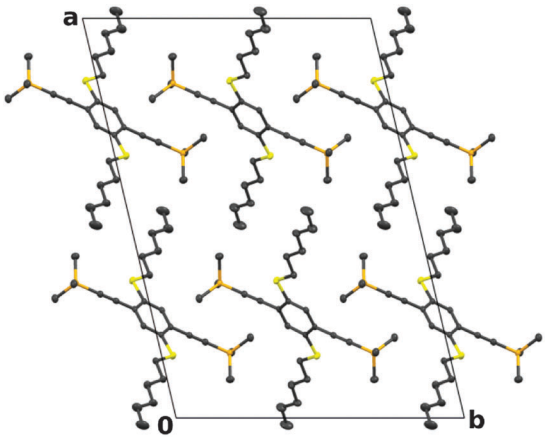

Fig. 1 Crystal structure of **6a** viewed down [010]. C, S and Si atoms are represented by gray, yellow and orange ellipsoids drawn at 50% probability levels, respectively. H atoms were omitted for clarity.

The crystal structures of **6a**[18] and **6b**[18] are isostructural and possess *C*2/*c* symmetry. One crystallographically unique molecule is located on a center of inversion. The hexyl chains extend in the plane of the benzene ring. Indeed, with the exception of the TMS groups the molecules are virtually flat: the largest distance of a non-H atom with the exception of the TMS-methyl groups to the least squares plane defined by the atoms of the π-conjugated core is 0.0958(13) Å (**6a**) and 0.121(3) Å (**6b**). The terminal atoms of the hexyl chain feature enlarged atomic displacement parameters, indicating static or dynamic disorder as expected for long alkyl chains. The molecules are arranged in a three dimensional network controlled solely by van der Waals interactions. As expected, the unit cell volume of **6b** is slightly larger than **6a** (3164.8(8) *vs.* 3085.8(3) Å^3) due to the additional space required for the Se atom.[18]

6d[18] (crystals were grown by solvent evaporation from ethanol) crystallizes in space group $P2_1/c$. Although, like in **6a** and **6b**, the molecules are located on centers of inversion, **6d** is structurally unrelated to the former. Most notably, the hexyl chains in **6d** propagate nearly perpendicular to the plane of the benzene ring. They are located in the pockets of the structure and the three terminal aliphatic C atoms feature disorder.

Electrochemical and photophysical properties of **6a–d** were probed by cyclic voltammetry (CV) as well as photometry (UV-vis absorption). CV revealed similar HOMO energy levels for compounds **6a** (−5.35 eV) and **6b** (−5.31 eV), whereas tellurium compound **6c** showed a significantly higher HOMO energy level of −5.08 eV. This fact is also indicated by decomposition of **6c** in DCM solution in contrast to **6a** and **6b**. DFT calculations performed did not reproduce the observed higher HOMO level for **6c**; however, a similar phenomenon for tellurium based compounds has been described in the literature.[19]

UV-vis absorption spectra of **6a–c** are depicted in Fig. 2 (right). The high wavelength absorption bands of **6a–c** are broad weak peaks, which are characteristic for n → π* transitions. The bands below 320 nm are attributed to π → π* transitions, given their spectral shape (vibronic structures) and intensity. The optical bandgaps were determined from the absorption onsets (Table 1).

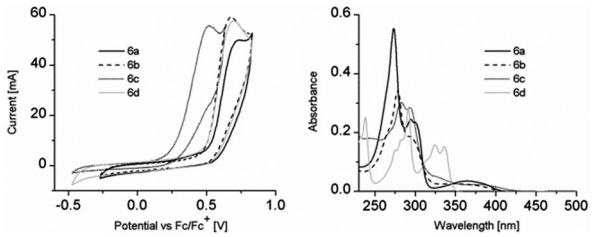

Fig. 2 CV charts of irreversible oxidation (left) and UV-vis absorption spectra (right) of **6a–d**.

Table 1 Photophysical and electrochemical data for **6a–d**

	E_{ox}[a] [V]	$\lambda_{on\text{-}set}$[b] [nm]/optical bandgap [eV]	HOMO level[c] [eV]
6a	0.55	406/3.05	−5.35
6b	0.51	408/3.04	−5.31
6c	0.28	425/2.92	−5.08
6d	0.51	347/3.57	−5.31

[a] Onset potential *vs.* Fc/Fc^+. [b] Absorption onset wavelength. [c] From CV on the premise that the Fc/Fc^+ energy level is −4.80 eV.

Similar values for the optical bandgap have been observed for **6a** and **6b**, indicating only a minor influence of the S–Se exchange on photophysical properties. In contrast, for compound **6c** a slightly reduced bandgap was observed.

The characterization of **6d** by CV and absorption measurements revealed a minor influence on the HOMO energy levels (−5.31 eV), but significant changes in the absorption spectra with a blue-shift of the absorption onset of ~60 nm/~0.5 eV compared to **6a** (Fig. 2). The marginal shift of the HOMO level indicates a minor conjugation between the heteroatom groups and the π-system of the benzene, which was also observed for the selenium derivative **6b**. The blue-shift is explained by the elimination of the lone pair electrons and, thus, the lack of n → π* transitions. The π → π* transition of **6d** (320–350 nm) is red-shifted by ~30 nm compared to **6a**, indicating a reduced π–π* bandgap.

To outline the effect of selective oxidation on material properties post-polymerization modification[20] was chosen as a proof of concept (Scheme 3). Polymer **8** was obtained by microwave-assisted Cu(I)-catalyzed azide–alkyne cycloaddition (CuAAC) polymerization of **6a** and **7**. The optimized procedure allows for *in situ* deprotection of **6a** and significantly reduces reaction times compared to conventional CuAAC polymerization.[10]

The oxidation of **8** was performed in analogy to the model reaction towards **6d**. Indeed, post-polymerization modification was accomplished quantitatively yielding polymer **9** (conversion monitored by ^1H NMR spectroscopy). Since acetone is the only by-product of the oxidation using DMDO, **9** was simply purified by solvent evaporation.

GPC measurements of both **8** and **9** indicate no degradation of the polymers during oxidation. While the number average molecular weight slightly decreased from 3.6 kDa to 3.5 kDa, the weight average molecular weight increased from 7.2 kDa to 7.5 kDa. These variations are within the limitations of the chosen relative method for molecular weight determination.

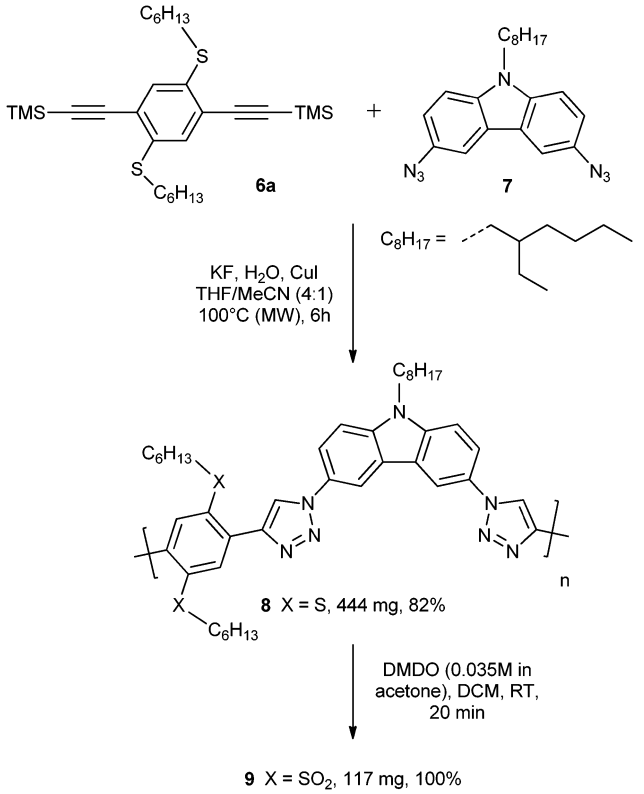

Scheme 3 Microwave-assisted CuAAC polymerization towards **8** and post-polymerization modification (oxidation) yielding **9**.

The effects of post-polymerization modification were evaluated by absorption and fluorescence measurements for polymers **8** and **9**.

Despite the drastic structural and electronic modification, converting the electron donating into an electron withdrawing substituent, qualitatively similar absorption characteristics but reduced absorbance values were observed (Fig. 3, left). In contrast, the fluorescence characteristics alter significantly shifting the emission maximum from 438 nm (**8**) to 516 nm (**9**). This severe red-shift of ~80 nm changes the emission color from blue to yellow (Fig. 3, right) suggesting a variety of potential applications

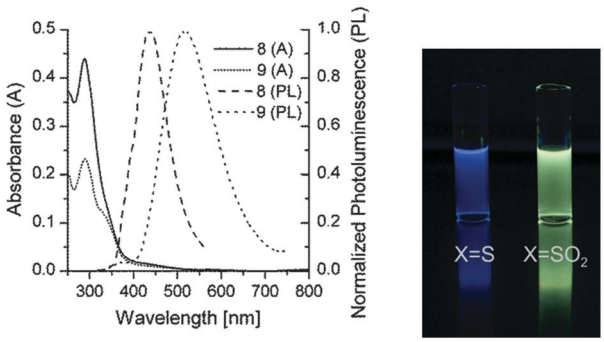

Fig. 3 UV-vis absorption and photoluminescence spectra of **8** (λ_{ex} = 288 nm) and **9** (λ_{ex} = 287 nm) (left), solutions of **8** (blue) and **9** (yellow) in DCM at λ_{ex} = 366 nm (right).

such as specific color tuning in the field of OLEDs, new strategies for device processing, *etc.* Further experimental and photophysical investigations are currently performed to analyze this effect and to prove the general applicability of this approach. Determination of quantum yields using an Ulbricht sphere afforded similar values of 13% and 15% for polymers **8** and **9**, respectively.

In conclusion, we have established a straightforward, cheap and reliable synthesis of versatile building blocks **6a–c** on a (multi)gram-scale. The application of the developed building blocks potentially yields functional organic materials with entirely new properties compared to widely applied 1,4-bis[(trimethylsilyl)-ethynyl]-2,5-bis(hexyloxy)benzene (X = O). Thus, microwave-assisted CuAAC polymerization of **6a** and post-polymerization modification were demonstrated. The observed alteration in photophysical properties by this simple oxidation procedure utilizing DMDO gives rise to several possible applications ranging from color tuning to post-processing modification of polymer layers.

Experimental section

General procedure for the synthesis of 6a–c

5 (1.0 eq.) was dissolved in degassed dry Et_2O (0.1 M) under an argon atmosphere in a pressure resistant glass vial. The solution was cooled to −78 °C and *t*-BuLi (1.7 M in pentane, 4.0 eq.) was slowly added. The resulting mixture was stirred for 45 min at −78 °C before allowing the solution to warm above 0 °C. Sulfur, selenium or dihexyltelluride (2.1 eq.) was then added and the yellow suspension was stirred for 3 h at room temperature/60 °C. If elemental reagents were used, hexyl iodide (2.2 eq.) was additionally added and the suspension was stirred at 60 °C overnight. The solution was poured into water and extracted three times with Et_2O. The combined organic layers were dried over anhydrous Na_2SO_4 and the solvent was removed *in vacuo*. The residue was purified by column chromatography (PE) or by crystallization from EtOH followed by trituration in boiling EtOH.

Microwave-assisted CuAAC polymerization

Dialkyne **6a** (1.0 eq.) and diazide **7** (1.0 eq.) were weighed in into separate vials. CuI (10 mol%), KF (3.0 eq.) and H_2O (8.0 eq.) were added to **6a** and the vial was sealed and flushed with argon. **7** was dissolved in degassed THF/MeCN (4 : 1, 0.15 M) and added to the other reagents *via* a syringe. The reaction mixture was then heated to 100 °C in the microwave-reactor for 6 h. The solution was added dropwise to methanol for precipitation and polymer **8** was collected by vacuum filtration.

Post-polymerization modification

Polymer **8** (1.0 eq.) was dissolved in DCM (0.008 M). DMDO (0.035 M in acetone, 4.2 eq.) was added dropwise and the solution stirred for 20 min at room temperature. Evaporation of the solvents yielded polymer **9**.

Acknowledgements

We gratefully thank H. Wutzel for performing GPC measurements and M. Taubländer for contributing to synthetic experiments. B. Holzer, E. Horkel and C. Hametner are acknowledged for performing NMR experiments.

Notes and references

1 M. C. Baier, J. Huber and S. Mecking, *J. Am. Chem. Soc.*, 2009, **131**, 14267–14273.
2 B. Liu, Y. Bao, H. Wang, F. Du, J. Tian, Q. Li, T. Wang and R. Bai, *J. Mater. Chem.*, 2012, **22**, 3555–3561.
3 A. Mangalum, R. J. Gilliard, Jr., J. M. Hanley, A. M. Parker and R. C. Smith, *Org. Biomol. Chem.*, 2010, **8**, 5620–5627.
4 S. He, A. A. Buelt, J. M. Hanley, B. P. Morgan, A. G. Tennyson and R. C. Smith, *Macromolecules*, 2012, **45**, 6344–6352.
5 S.-S. Jester, N. Shabelina, B. S. M. Le and S. Höger, *Angew. Chem., Int. Ed.*, 2010, **49**, 6101–6105.
6 A. Fuerstner, *Angew. Chem., Int. Ed.*, 2013, **52**, 2794–2819.
7 G. Brizius, N. G. Pschirer, W. Steffen, K. Stitzer, H.-C. zur Loye and U. H. F. Bunz, *J. Am. Chem. Soc.*, 2000, **122**, 12435–12440.
8 V. S. Y. Lin, D. R. Radu, M.-K. Han, W. Deng, S. Kuroki, B. H. Shanks and M. Pruski, *J. Am. Chem. Soc.*, 2002, **124**, 9040–9041.
9 J. Huber, C. Jung and S. Mecking, *Macromolecules*, 2012, **45**, 7799–7805.
10 Z. Chen, D. R. Dreyer, Z.-Q. Wu, K. M. Wiggins, Z. Jiang and C. W. Bielawski, *J. Polym. Sci., Part A: Polym. Chem.*, 2011, **49**, 1421–1426.
11 M. T. Dang, L. Hirsch and G. Wantz, *Adv. Mater.*, 2011, **23**, 3597–3602.
12 Z. Chen, H. Lemke, S. Albert-Seifried, M. Caironi, M. M. Nielsen, M. Heeney, W. Zhang, I. McCulloch and H. Sirringhaus, *Adv. Mater.*, 2010, **22**, 2371–2375.
13 A. A. Jahnke and D. S. Seferos, *Macromol. Rapid Commun.*, 2011, **32**, 943–951.
14 P. López-Alvarado, C. Avendaño and J. C. Menéndez, *Synth. Commun.*, 2002, **32**, 3233–3239.
15 V. B. Van, K. Miki and T. M. Swager, *Org. Lett.*, 2010, **12**, 1292–1295.
16 J. M. Oliveira, J. C. R. Freitas, J. V. Comasseto and P. H. Menezes, *Tetrahedron*, 2011, **67**, 3003–3009.
17 H. Mikula, D. Svatunek, D. Lumpi, F. Glöcklhofer, C. Hametner and J. Fröhlich, *Org. Process Res. Dev.*, 2013, **17**, 313–316.
18 See ESI† for details.
19 K. Takimiya, Y. Konda, H. Ebata, N. Niihara and T. Otsubo, *J. Org. Chem.*, 2005, **70**, 10569–10571.
20 M. A. Gauthier, M. I. Gibson and H.-A. Klok, *Angew. Chem., Int. Ed.*, 2009, **48**, 48–58.

